Ternary III−As Antimonide

Subjects: Nanoscience & Nanotechnology

Contributor: Ezekiel Anyebe

During the last few years, there has been renewed interest in the monolithic integration of gold-free, Ternary III–As Antimonide (III–As–Sb) compound semiconductor materials on complementary metal-oxide-semiconductor (CMOS)—compatible silicon substrate to exploit its scalability, and relative abundance in high-performance and cost-effective integrated circuits based on the well-established technology. Ternary III–As–Sb nanowires (NWs) hold enormous promise for the fabrication of high-performance optoelectronic nanodevices with tunable bandgap. However, the direct epitaxial growth of gold-free ternary III–As–Sb NWs on silicon is extremely challenging, due to the surfactant effect of Sb.

Ternary III−As Antimonide

1. Introduction

1.1. Ternary III–As–Sb Nanowires

In recent years, ternary III−As Antimonide (III–As–Sb) materials have increasingly attracted enormous interest as potential building blocks for next-generation optoelectronics. Among these, the InAsSb and GaAsSb alloys, have particularly attracted increasing attention, due to their intriguing and promising properties. The InAsSb material possesses a tunable bandgap, enabling bandgap engineering for controlled characteristics and device application with its direct bandgap having the smallest energy among all the entire III–V semiconductors (145 meV for $x = 0.63$ at 0 K)[1][2]. It's potential to extend the detection wavelength limit of InAs (3.8 µm) to the long-wavelength infrared range (LWIR) (8–12 µm)[3] has attracted enormous interest for diverse applications, including photodetectors as a potential replacement to existing HgCdTe-based infrared LWIR detectors which is plagued by concerns of toxicity[4], surface instability, high growth, and processing cost, as well as non-uniformity[5]. In addition, Sb incorporation in InAs opens up opportunities for the investigation of important material-related properties, such as spin-orbit coupling and quantum confinement[2], as well as increases the minority carrier lifetime and mobility[6], enabling highly efficient field-effect transistors. The InAsSb material also offers several advantages, including low electron effective mass, high mobility at room temperature, and reduced auger recombination rate (auger coefficient as low as 10^{-7} cm^6/s)[7]. On the other hand, the ternary GaAsSb alloy possesses a wavelength covering a highly important range from the near IR (0.87 µm for GaAs) to the mid-IR (1.7 µm for GaSb) region, which holds enormous potential for applications in optoelectronic devices, including optical telecommunications, quantum information science, solar cells, and infrared photodetectors[8][9].

During the last few years, there has been renewed enthusiasm in the monolithic integration of Ternary III–As–Sb compound semiconductors on complementary metal-oxide-semiconductor (CMOS)—compatible silicon substrate to exploit the fascinating properties of the former, including direct bandgap, exceptional optical properties, and high carrier mobility, as well as the scalability, availability and high-quality of silicon to enable application in high-performance, cost-effective devices and integrated circuits based on the well-established Si technology. However, the epitaxial growth of III–V semiconductors on Si is challenging owing to large differences in lattice mismatch, thermal expansion coefficient, and crystal structure (whereas III–Vs have a zinc blende or wurtzite structure, Si has a covalent diamond structure)[10], as well as the polar/nonpolar nature of semiconductors/Si substrate[11] which often results in strain-induced defects and degradation of material quality[12]. One-dimensional nanowires (NWs) provide the panacea for the integration of these materials directly on highly mismatched substrates. The small footprint of NWs in contact with the substrate could be exploited to evade the strict lattice matching requirements for the growth III–V semiconductor thin-film on highly lattice-mismatched substrates, due to elastic strain relaxation enabling the monolithic integration of NWs on silicon. The heteroepitaxial growth of high-quality III–V–Sb NWs directly on Si substrates would undoubtedly open the flood gates for the experimental study of the band structure, carrier transport, and other important fundamental properties of III–As–Sb/Si heterojunctions which are not readily available in conventional thin-film structures[13][14]. In addition, it would enable the independent control of the NWs geometry for optimal device functionality[15]. However, the nucleation and growth of III–As–Sb NWs directly on substrates is extremely challenging[16] and requires strict compliance with contact angle requirements[17][18] owing to the surfactant effect of Sb on the substrate. As an alternative, previous ground-breaking research that provided great insight into the growth of Sb-based NWs, utilized NWs stems, such as InAs[12][19] and InP[2], to facilitate vertical NW directionality. More so, the growth of GaAsSb ternary alloy is particularly made more difficult, due to the existence of a large miscibility gap, $0.25 < x < 0.7$[20]. Furthermore, Au (which is the most commonly used catalyst) is incompatible with CMOS processing[21] and could potentially result in the unintentional incorporation of impurities which adversely degrade NWs properties, a phenomenon which has mitigated its potential for use in the monolithic integration of semiconductor NWs with silicon.

This paper provides a detailed review of CMOS compatible, Au-free growth, and optoelectronic applications of Ternary III–As–Sb NWs directly on Si, specifically InAsSb and GaAsSb NWs. We do not attempt to explicitly cover all III–Sb NWs grown on III–V substrates, NWs stems and axial heterostructures, etc., which are inclusive of Au-catalyzed NWs. Broad and more general reviews encompassing the growth of such Sb-based NWs can be found elsewhere[18][22][23][24][25]. First, a comprehensive review of recent progress made in the Au-free growth of InAsSb and GaAsSb NWs directly on Si is presented, followed by a detailed description of the Sb surfactant effect and its influence on both NWs morphology and structure of Ternary III–As–Sb NWs. Then, the various strategies that have been successfully deployed for the suppression of the Sb surfactant effect are highlighted. Finally, recent advances made in the development of CMOS compatible, Ternary III–As–Sb NWs-based devices are explicated.

2. Growth of Au-Free Ternary III–As–Sb Nanowires Directly on Silicon

To monolithically integrate highly efficient Ternary III–V–Sb NWs-based devices (such as infrared detectors) with the Si-based read-out circuit[26], NWs have to be directly grown on the Si substrate. During the last few years, significant progress has been made on the Au-free growth of ternary III–V–Sb NWs directly on silicon using various growth methods, including MBE, MOCVD, MOVPE, and CBE. Here, we summarize the recent progress made in the growth of InAsSb and GaAsSb NWs directly on silicon.

2.1. InAsSb Nanowires Growth Directly on Silicon

There is an extensive body of literature on the growth of Au-catalyzed heterostructured InAs/InAsSb[27][28] and InAsSb NWs on InAs(111)B substrate[12]; however, the first successful growth of InAsSb NWs directly on Si (111) was demonstrated by Du et al. [29] in 2013, via the self-seeded growth mechanism by MOVPE. The Sb content was found to have a significant effect on the morphology and crystal quality of the NWs. The length of NWs decreased from (0.15–0.60) µm to (0.39–0.07) µm while the diameter increased from (27–65) nm to (434–698) nm with increasing Sb vapor phase composition (x_v) from 0 to 0.8 [where x_v is the ratio of Sb to the combined (As and Sb) group-V material flux]. Short and thick flat pillars were obtained after 2 min of growth at the highest Sb composition (x_{sb}) of 43 at.%. This implies an increase in x_v translates to an enhancement of radial growth with suppression of axial growth. In 2014, our research group[30] also realized the growth of InAsSb NWs on bare Si by MBE via an In-assisted nucleation without using NWs stems. It was observed that the geometry of the NWs was modified by increasing x_v with an almost doubling of the lateral dimension and a corresponding suppression in NWs axial growth, which is similar to the earlier observation by Du et al.[31]. Several important milestones were achieved in 2015, as there was increased research on the growth of InAsSb directly on Si. Motivated by the observed influence of Sb addition to the geometry of InAsSb NWs, our research group investigated the surfactant effect of Sb addition to the MBE growth of NWs [32] and Sb induced phase control[33]. It was confirmed that trace Sb flux has the potential of tuning the geometry of InAsSb NWs by promoting lateral growth while suppressing axial growth. The observed behavior is attributed to the surfactant effect of Sb, which results in modifications to the kinetic and thermodynamic processes. A thermodynamic mechanism that accounts for Sb segregation in InAsSb NWs was thus elucidated, unraveling a new route towards precisely controlled NW morphology by the addition of Sb (more discussion on this to follow in subsequent sections). Another important step towards a better understanding of the growth of this ternary material was achieved in 2015 when Du et al. [32] fabricated InAsSb NWs on Si (111) substrate by MOVPE as a function of various growth conditions, including V/III ratio, group Sb flow rate fraction, and temperature. They found that InAsSb NWs can display both vapor–liquid–solid (VLS) and vapor–solid (VS) growth mechanism depending on the growth parameters. At low V/III ratio and relatively high Sb flow rate fraction, the VLS growth mechanism is dominant, whereas, at high V/III ratio and relatively low Sb flow rate fraction, NWs were grown via the VS mechanism. There were marked differences in morphology, Sb content, growth direction, and crystal quality of as-grown NWs depending on the growth mechanism, as depicted in Figure 1. The authors observed that the VS grown NWs exhibited uniform growth direction and diameter, with a hexagonal cross section. In addition, the NWs tips were flat with no droplets present, suggesting a catalyst-free growth mechanism with uniform Sb distribution, which is beneficial for device integration of NWs array. Conversely, the VLS grown NWs are almost kink-free and display multiple orientations. The NW top terminates with a hemispherical In–Sb alloy droplet indicative of a catalyst-assisted growth mechanism with significant variation in Sb distribution and display of a pure

crystal phase, which was mainly attributed to the In-rich droplets that are advantageous for the development of single NW devices. This work demonstrates that the In-rich droplet of the Au-free growth could potentially improve the crystal quality of ⟨111⟩-oriented NWs without the introduction of impurities. The growth temperature regime for realizing InAsSb NWs was identified to be in the range of 450–510 °C at an x_v of 0.2. In addition, the authors observed an inverse relationship between the lateral growth rate of the NWs and growth temperature, with higher growth temperatures favoring axial NWs growth.

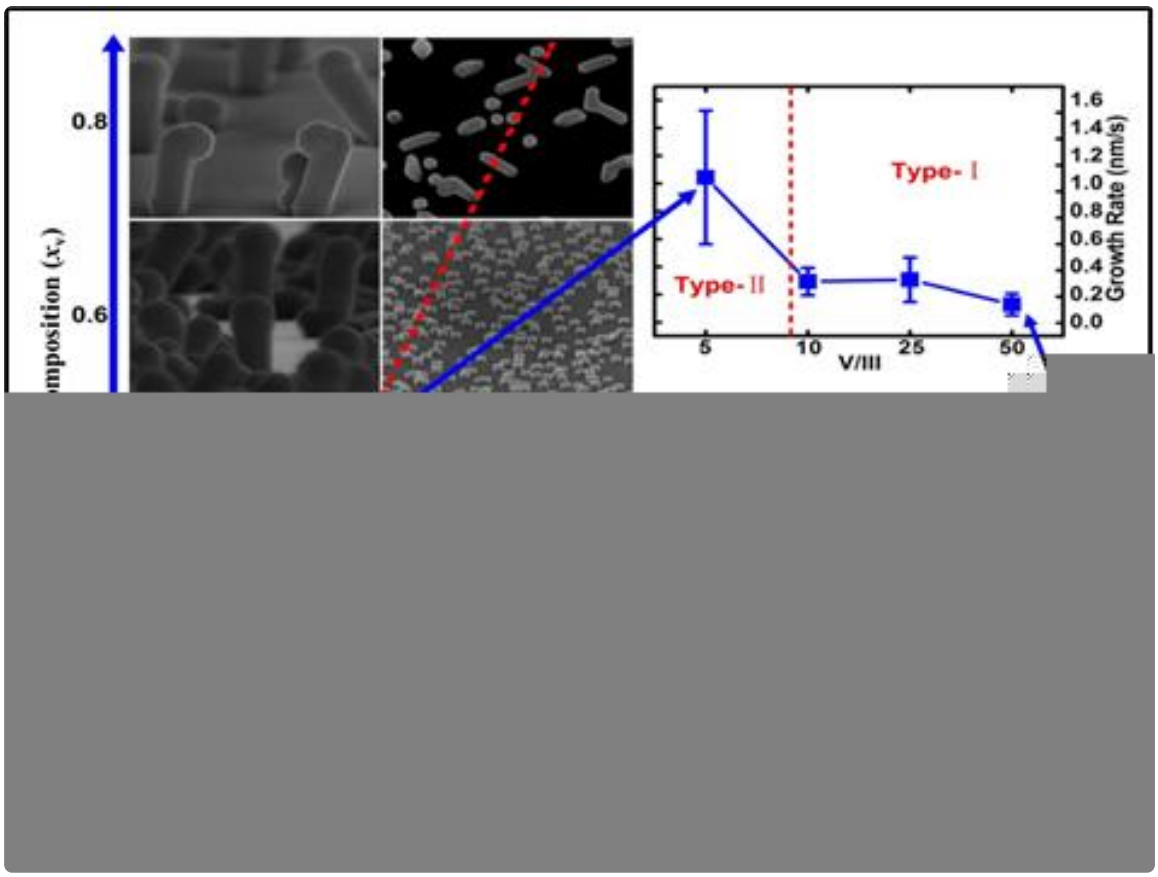

Figure 1. Images of InAsSb NWs as a function of x_v and V/III ratio. The inset in the top right shows the variation of growth rate with the V/III ratio for x_v = 0.4 (as highlighted by the blue rectangular frame). The solid line is used for eye guide, indicating the changing trend of growth rate. The red dashed line in the figure indicates the transition boundary between vapor–solid and vapor–liquid–solid growth modes. Reproduced with permission from[32]; Copyright 2015, American Chemical Society.

In 2020, Wen et al. [34] investigated the influence of essential growth parameters of growth temperature, indium flux, and substrate type on the growth of silver-assisted $InAs_{1-x}Sb_x$ NWs directly grown on Si (111) substrates by MBE. The authors observed the growth of vertically aligned $InAs_{1-x}Sb_x$ NWs directly on Si (111) substrates is extremely difficult; however, the use of relatively high growth temperature and low indium fluxes promotes the growth of vertically aligned NWs with a corresponding suppression in random growth of NWs. On the other hand, the growth of non-[111]-orientation NWs, NWs tapering, and number density was found to increase with increasing In-flux, due to higher indium content resulting in increased segregation of the silver-indium catalyst on the top of the NW during growth. A further increase in Indium composition and catalyst segregation results in a gradual

decrease in catalyst diameter, leading to enhanced tapering, since NWs diameter is highly dependent on the size of the catalyst alloy. There was no obvious variation in the morphology and growth direction of the InAs0.85Sb0.15 NWs grown on various Si (111), Si (110), and Si (100) substrates, which were all characterized by the growth of non-[111]-oriented NWs and attributed to the formation of an ultrathin oxide layer on the silicon surface prior to loading into the MBE chamber.

2.2. GaAsSb Nanowires Growth Directly on Silicon

Building on the pioneering Au-assisted growth of GaAsSb NWs on GaAs(111)B by Dheeraj et al. [35] in 2008, previous Au-free GaAsSb NWs growth on Si were limited to heterostructures[36][37]. To the best of our knowledge, the first reported Au-free growth of GaAsSb NWs directly on Si was reported in 2013 by Alarcon-Llad´o et al.[38], who systematically investigated the optical properties of MBE grown NWs for Sb contents from 0 to 44 at.%, as determined by EDX and provided a reference for the study of ternary NWs alloys while demonstrating the high-quality of gold-free ternary antimonide NWs directly grown on silicon. This report was followed in 2014 by the selective area, MBE growth of Pure zinc blende GaAsSb NWs by the same group[39]. The authors unambiguously demonstrated that the NWs are completely twin-free down to the first bilayer with three-dimensional composition evolution. This work opened the way for the integration of novel infrared nanodevices directly on the cost-effective Si platform. Li et al.[40] systematically investigated Ga-catalyzed, MBE growth of GaAsSb NWs by tuning the Sb and As fluxes achieve near full-composition-range. By tuning the Sb flux from 4.50×10^{-7} to 1.43×10^{-6} Torr the Sb content increased from 0.18 to 0.35 (Figure 2a–c), with almost no NWs growth, realized on the Si substrates for $x > 0.45$ with limited growth of short and thick NWs. However, by increasing the Sb content from $x = 0.30$ to 0.60, both the density and axial growth rate of the GaAsSb NWs were decreased while the diameter increased, and No NWs growth was realized for a high Sb content of 0.75 at.% (Figure 2f) which was rather dominated by the growth of a two-dimensional film.

Figure 2. Side-view SEM images of the Ga self-catalyzed $GaAs_{1-x}Sb_x$ nanowires grown on Si (111) substrates by molecular beam epitaxy (MBE). (**a**–**c**) $GaAs_{1-x}Sb_x$ nanowires were obtained by increasing Sb flux, and the corresponding x_{sb} are 0.18, 0.27, and 0.35, respectively. (**d**–**f**) $GaAs_{1-x}Sb_x$ nanowires were obtained by reducing As flux, and the corresponding x_{sb} are 0.30, 0.60, and 0.75, respectively. Reproduced with permission from [60]; Copyright 2017, American Chemical Society.

A comprehensive study of the effect of Sb incorporation on the composition modulation, structural and optical properties of self-assisted GaAsSb NWs on (111) Si substrate was conducted by Ahmad et al.[41] in 2017 using MBE. The NWs exhibited a pure zinc blende crystal structure, largely free of any planar defects with inverse dependence of NWs density as a function of Sb flux, which was associated with the surfactant effect of Sb and droplet size-dependent Gibbs–Thomson effects[42]. EDX extracted Sb composition in as-grown GaAsSb axial NW varied from 2.8–16 at.%; however, higher Sb incorporation enhanced radial NWs growth with a concomitant reduction in the axial growth rate was observed. The authors revealed that thinner NWs with low Sb composition presents inhomogeneous Sb composition distribution radially with a depleted Sb surface region, whereas, NWs with larger NWs and higher Sb composition (16 at.%) display a more uniform Sb compositional distribution radially leading to type-I optical transitions. This variation in Sb distribution was attributed to differences in growth mechanism. In the same year, the influence of group V/III beam equivalent (BEP) ratios and substrate temperature on the density and chemical composition of self-catalyzed, MBE grown GaAsSb NWs on p-type Si (111) substrate was systematically Investigated[43]. A two-step growth temperature sequence of initiating growth at a relatively higher temperature and then continuing the growth at a lower temperature was shown to be a promising technique for realizing a high-density of NWs despite higher Sb compositions.

To engineer the optical and electrical properties of semiconductor NWs for various optoelectronic applications, it is important to precisely control essential growth parameters. In 2020, the influence of As_2 and As_4 species on the growth of self-catalyzed GaAsSb NWs was investigated by Koivusalo et al. [44] by MBE via a droplet epitaxy growth technique. The authors demonstrated that a careful selection of As species is critical for tuning the NW dimensions and the incorporation mechanism of Sb. It was shown that As_4 is the preferred candidate of choice when axial NWs growth is essential, whereas As_2 is the best alternative when radial growth is required. Although, the NWs grown using As_2 displayed a relatively larger diameter, As_4 counterparts grown under identical growth conditions were reported to be longer in length. As_4 mitigates Sb induced suppression of NW aspect ratio for enhanced axial growth while favoring the extension of the axial growth parameter window, to enable the growth of GaAsSb NWs with high (47%) Sb composition. The observed As_4 induced enhanced axial growth is associated with the As incorporation kinetics. As_4 has a lower sticking coefficient compared to As_2 on the common sidewall surface of self-catalyzed GaAs NWs. As a result, there is less efficiency As incorporation on the sidewall from As_4 compared to As_2 during VS growth, which implies an increase in local V/III ratio in the vapor phase with increased droplet supersaturation and axial NW growth rate. On the other hand, As_2 promotes sidewall nucleation for enhanced radial growth, due to its relatively high sticking coefficient.

References

1. Yen, M.Y.; People, R.; Wecht, K.W.; Cho, A.Y. Long-wavelength photoluminescence of InAs1−xSbx grown by molecular beam epitaxy on (100) InAs. Appl. Phys. Lett. 1988, 52, 489.
2. Claes, T.; Philippe, C.; Sébastien, P.; Kimberly, A.D. Electrical properties of InAs1−xSbx and InSb nanowires grown by molecular beam epitaxy. Appl. Phys. Lett. 2012, 100, 232105.
3. Rogalski, A. Infrared detectors: An overview. Infrared Phys. Technol. 2002, 43, 187–210.
4. Pea, M.; Ercolani, D.; Li, A.; Gemmi, M.; Rossi, F.; Beltram, F.; Sorba, L. Suppression of lateral growth in InAs/InAsSb heterostructured nanowires. J. Cryst. Growth 2013, 366, 8–14.
5. Rogalski, A. Infrared detectors: Status and trends. Prog. Quantum. Electron. 2003, 27, 59–210.
6. Olson, B.V.; Shaner, E.A.; Kim, J.K.; Klem, J.F.; Hawkins, S.D.; Murray, L.M.; Prineas, J.P.; Flatté, M.E.; Boggess, T.F. Time-resolved optical measurements of minority carrier recombination in a mid-wave infrared InAsSb alloy and InAs/InAsSb superlattice. Appl. Phys. Lett. 2012, 101, 92109.
7. Shao, H.L.W.; Torfi, A.; Moscicka, D.; Wang, W.I. Room-temperature InAsSb photovoltaic detectors for mid-infrared applications. IEEE Photonic Tech. L. 2006, 18, 1756–1758.
8. Li, Z.Y.; Yuan, X.M.; Fu, L.; Peng, K.; Wang, F.; Fu, X.; Caroff, P.; White, T.P.; Tan, H.H.; Jagadish, C. Room temperature GaAsSb single nanowire infrared photodetectors. Nanotechnology 2015, 26, 445202.
9. Li, Z.Y.; Yuan, X.M.; Gao, Q.; Yang, I.; Li, L.; Caroff, P.; Allen, M.; Allen, J.; Tan, H.H.; Jagadish, C.; et al. In situ passivation of GaAsSb nanowires for enhanced infrared photoresponse. Nanotechnology 2020, 31, 349601.
10. Mårtensson, T.; Svensson, C.P.T.; Wacaser, B.A.; Larsson, M.W.; Seifert, W.; Deppert, K.; Gustafsson, A.; Wallenberg, L.R.; Samuelson, L. Epitaxial III−V Nanowires on Silicon. Nano Lett. 2004, 4, 1987–1990.
11. Bolkhovityanov, Y.B.; Pchelyakov, O.P. GaAs epitaxy on Si substrates: Modern status of research and engineering. Physics 2008, 51, 437–456.
12. Borg, B.M.; Kimberly, A.D.; Joël, E.; Lars-Erik, W. Enhanced Sb incorporation in InAsSb nanowires grown by metalorganic vapor phase epitaxy. Appl. Phys. Lett. 2011, 98, 113104.
13. Wei, W.; Bao, X.Y.; Soci, C.; Ding, Y.; Wang, Z.L.; Wang, D. Direct Heteroepitaxy of Vertical InAs Nanowires on Si Substrates for Broad Band Photovoltaics and Photodetection. Nano Lett. 2009, 9, 2926–2934.
14. Cantoro, M.; Wang, G.; Lin, H.C.; Klekachev, A.V.; Richard, O.; Bender, H.; Kim, T.G.; Clemente, F.; Adelmann, C.; Veen, M.H.V.D.; et al. Large-area, catalyst-free heteroepitaxy of InAs nanowires on Si by MOVPE. Phys. Status Solidi A 2011, 208, 129–135.

15. Caroff, P.; Messing, M.E.; Borg, B.M.; Dick, K.A.; Deppert, K.; Wernersson, L.-E. InSb heterostructure nanowires: MOVPE growth under extreme lattice mismatch Nanotechnology 2009, 20, 495606.
16. Lorenzo, L.; Daniele, E.; Fabio, B.; Lucia, S. Growth mechanism of InAs–InSb heterostructured nanowires grown by chemical beam epitaxy. J. Cryst. Growth 2011, 323, 304–306.
17. Nebol'sin, V.A.; Shchetinin, A.A. Role of surface energy in the vapor-liquid-solid growth of silicon. Inorg. Mater. 2003, 39, 899–903.
18. Borg, B.M.; Wernersson, L.E. Synthesis and properties of antimonide nanowires Nanotechnology 2013, 24, 202001.
19. Sourribes, M.J.L.; Isakov, I.; Panfilova, M.; Liu, H.; Warburton, P.A. Mobility Enhancement by Sb-mediated Minimisation of Stacking Fault Density in InAs Nanowires Grown on Silicon. Nano Lett. 2014, 14, 1643–1650.
20. Stringfellow, G.B. Spinodal decomposition and clustering in III/V alloys. J. Electron. Mater. 1982, 11, 903–918.
21. Allen, J.E.; Hemesath, E.R.; Perea, D.E.; Lensch-Falk, J.L.; Li, Z.Y.; Yin, F.; Gass; M.H.; Wang, P.; Bleloch, A.L.; Palmer, R.E.; et al. High-resolution detection of Au catalyst atoms in Si Nanowires. Nat. Nanotechnol. 2008, 3, 168–173.
22. SenPo, Y.; Lifan, S.; Johnny, C.H. Recent advances in III–Sb nanowires: From synthesis to applications Nanotechnology 2019, 30, 202003.
23. Gao, Z.; Sun, J.; Han, M.; Yin, Y.; Gu, Y.; Yang, Z.X.; Zeng, H. Recent advances in Sb-based III–V nanowires. Nanotechnology 2019, 30, 212002.
24. Dingding, R.; Lyubomir, A.; Antonius, T.J.V.H.; Helge, W.; Bjørn-Ove, F. Epitaxially grown III–arsenide–antimonide nanowires for optoelectronic applications. Nanotechnology 2019, 30, 294001.
25. Boras, G.; Yu, X.; Liu, H. III–V ternary nanowires on Si substrates: Growth, characterization and device applications. J. Semicond. 2019, 40, 101301.
26. Besikci, C. III–V infrared detectors on Si substrates.Proc. SPIE 2000, 3948, 31–39.
27. Xu, T.; Dick, K.A.; Plissard, S.; Nguyen, T.H.; Makoudi, Y.; Berthe, M.; Nys, J.P.; Wallart, X.; Grandidier, B.; Caroff, P. Faceting, composition and crystal phase evolution in III–V antimonide nanowire heterostructures revealed by combining microscopy techniques. Nanotechnology 2012, 23, 95702.
28. Ercolani, D.; Gemmi, M.; Nasi, L.; Rossi, F.; Pea, M.; Li, A.; Salviati, G.; Beltram, F.; Sorba, L. Growth of InAs/ InAsSb heterostructured nanowires. Nanotechnology 2012, 23, 115606.

29. Du, W.-N.; Yang, X.-G.; Wang, X.-Y.; Pan, H.-Y.; Ji, H.-M.; Luo, S.; Yang, T.; Wang, Z.-G. The self-seeded growth of InAsSb nanowires on silicon by metal-organic vapor phase epitaxy. J. Cryst. Growth 2014, 396, 33–37.
30. Anyebe, E.A.; Zhuang, Q. Self-catalysed InAs1−XSbx nanowires grown directly on bare Si substrates. Mater. Res. Bull. 2014, 60, 572–575.
31. Du, W.-N.; Yang, X.-G.; Wang, X.-Y.; Pan, H.-Y.; Ji, H.-M.; Luo, S.; Yang, T.; Wang, Z.-G. The self-seeded growth of InAsSb nanowires on silicon by metal-organic vapor phase epitaxy. J. Cryst. Growth 2014, 396, 33–37
32. Du, W.; Yang, X.; Pan, H.; Wang, X.; Ji, H.; Luo, S.; Ji, X.; Wang, Z.;Yang, T. Two Different Growth Mechanisms for Au-Free InAsSb Nanowires Growth on Si Substrate. Cryst. Growth Des. 2015, 15, 2413−2418.
33. Zhuang, Q.D.; Anyebe, E.A.; Chen, R.; Liu, H.; Sanchez, A.M.; Rajpalke, M.K.; Veal, T.D.; Wang, Z.M.; Huang, Y.Z.; Sun, H.D. Sb-Induced phase control of InAsSb nanowires grown by molecular beam epitaxy. Nano Lett. 2015, 15, 1109−1116.
34. Wen, L.; Liu, L.; Liao, D.; Zhuo, R.; Pan, D.; Zhao, J. Silver-assisted growth of high-quality InAsSb
35. Dheeraj, D.L.; Patriarche, G.; Largeau, L.; Zhou, H.L.; van Helvoort, A.T.J.; Glas, F.; Harmand, J.C.; Fimland, B.O.; Weman, H. Zinc blende GaAsSb nanowires grown by molecular beam epitaxy. Nanotechnology 2008, 19, 275605.
36. Plissard, S.; Dick, K.A.; Wallart, X.; Caroff, P. Gold-free GaAs/GaAsSb heterostructure nanowires grown on silicon. Appl. Phys. Lett. 2010, 96, 121901.
37. Munshi, A.M.; Dheeraj, D.L.; Todorovic, J.; van Helvoort, A.T.J.; Weman, H.; Fimland, B.-O. Crystal phase engineering in self-catalyzed GaAs and GaAs/GaAsSb nanowires grown on Si(111). J. Cryst. Growth 2013, 372, 163–169.
38. Alarcón-Lladó, E.; Conesa-Boj, S.; Wallart, X.; Caroff, P.; Morral, A.F.I. Raman spectroscopy of self-catalyzed GaAs1−xSbx nanowires grown on silicon. Nanotechnology 2013, 24, 405707.
39. Conesa-Boj, S.; Kriegner, D.; Han, X.-L.; Plissard, S.; Wallart, X.; Stangl, J.; Morral, A.F.I.; Caroff, P. Gold-Free Ternary III–V Antimonide Nanowire Arrays on Silicon: Twin-Free down to the First Bilayer. Nano Lett. 2014, 14, 326–332.
40. Li, L.; Pan, D.; Xue, Y.; Wang, X.; Lin, M.; Su, D.; Zhang, Q.; Yu, X.; So, H.; Wei, D.; et al. Near Full-Composition-Range High-Quality GaAs1–xSbx Nanowires Grown by Molecular-Beam Epitaxy. Nano Lett. 2017, 17, 622–630.
41. Ahmad, E.; Ojha, S.K.; Kasanaboina, P.K.; Reynolds Jr, C.L.; Liu, Y.; Iyer, S. Bandgap tuning in GaAs1–xSbx axial nanowires grown by Ga-assisted molecular beam epitaxy. Semicond. Sci. Technol. 2017, 32, 035002.

42. Dubrovskii, V.G.; Sibirev, N.V.; Cirlin, G.E.; Soshnikov, I.P.; Chen, W.H.; Larde, R.; Cade, E.I.; Pareige, P.; Xu, T.; Grandidier, B.; et al. Gibbs-Thomson and diffusion-induced contributions to the growth rate of Si, InP, and GaAs nanowires. Phys. Rev. B 2009, 79, 205316.
43. Ahmad, E.; Karim, M.R.; Hafiz, S.B.; Reynolds, C.L.; Liu, Y.; Iyer, S.A. Two-Step Growth Pathway for High Sb Incorporation in GaAsSb Nanowires in the Telecommunication Wavelength Range. Sci. Rep. 2017, 7, 1–12.
44. Koivusalo, E.; Helder, J.; Galeti, H.V.A.; Gobato, Y.G.; Guina, M.; Hakkarainen, T. The role of As species in self-catalyzed growth of GaAs and GaAsSb nanowires. Nanotechnology 2020, 202031, 465601.